Applied Catalysis B: Environmental 90 (2009) 1–9

Contents lists available at ScienceDirect

Applied Catalysis B: Environmental

journal homepage: www.elsevier.com/locate/apcatb

Review

Supported bimetallic AuRh/γ-Al_2O_3 nanocatalyst for the selective catalytic reduction of NO by propylene

Licheng Liu, Xiao Guan, Zhimei Li, Xuehong Zi, Hongxing Dai, Hong He *

Laboratory of Catalysis Chemistry and Nanoscience, Department of Chemistry and Chemical Engineering, College of Environmental and Energy Engineering, Beijing University of Technology, No. 100 Pingleyuan, Chaoyang District, Beijing 100124, China

ARTICLE INFO

Article history:
Received 5 November 2008
Received in revised form 23 February 2009
Accepted 26 February 2009
Available online 13 March 2009

Keywords:
Nanocatalyst
Rhodium
Gold
Selective catalytic reduction
Nitrogen monoxide

ABSTRACT

A new method entitled Ultrasound-assisted Membrane Reduction (UAMR) was developed to prepare highly dispersed monometallic Rh/γ-Al_2O_3 and bimetallic AuRh/γ-Al_2O_3 catalysts. In this process, the reductant ($NaBH_4$) solution is infiltrated through ceramic membrane tubes to a flowing suspension mixture of noble metal precursors and γ-Al_2O_3, and then the noble metal ions were reduced and deposited on the γ-Al_2O_3 to form nanoparticles or clusters on the surface of the carrier. The smaller noble metal nanoparticles (~5 nm) and higher activity for the selective catalytic reduction (SCR) of NO by propylene at low temperature were obtained over the catalysts prepared by the new method, compared to the catalysts prepared by conventional impregnation method. The AuRh/γ-Al_2O_3 catalyst with 0.33 wt% Au and 0.17 wt% Rh (M_{Rh}:M_{Au} = 1:1) loading exhibited higher propylene and NO conversions but lower NO conversion to N_2 than 0.5 wt% Rh/γ-Al_2O_3 catalyst, both of which were fabricated by the new preparation process. The stronger NO adsorption capability and formation of surface nitrates were validated over bimetallic AuRh/γ-Al_2O_3 catalysts in NO-TPD experiment. The synergistic effect of bimetallic system could improve the performance of SCR of NO and reduce the cost for platinum group metals based catalysts.

Contents

1. Introduction

The selective catalytic reduction (SCR) of nitrogen oxides (NO_x) by hydrocarbons (HC) has received great attention as a potentially effective method to eliminate NO_x in the exhausted emissions from lean-burn gasoline and diesel fueled vehicles [1–4]. The reaction

* Corresponding author. Fax: +86 10 67396588.
E-mail address: hehong@bjut.edu.cn (H. He).

0926-3373/$ – see front matter © 2009 Elsevier B.V. All rights reserved.
doi:10.1016/j.apcatb.2009.02.022

has been studied intensively over several types of catalysts in the presence of excess oxygen, such as zeolite-based materials [5–8], base metal oxides supported on oxides (e.g. alumina) [9–11], supported noble metals catalysts, in particular platinum group metals (PGMs) [12–17]. A number of critical reviews have focused on the SCR of NO_x by hydrocarbons [18–24]. Compared with other catalysts, supported noble metal catalysts exhibit rather high activity for SCR reaction at relatively low temperature and enhanced resistance against water and sulphur [13,17,25]. Many published presentations have devoted to the study of selective reduction of NO_x over Rh-based catalysts [16,17,23]. The investigation results revealed that Rh catalysts showed superior selectivity to N_2 in NO_x reduction in spite of lower activity at low temperature compared to other PGMs (e.g. Pt) among the noble metal based catalysts [17].

It is well known that the noble metals of Pt, Rh, and Pd are essentially active components in the widespread available three-way catalysts [26,27]. However, the rapid increment of automobile production has resulted in the augment of consumption and prices of such noble metals, especially for the Rh [27]. This status forces people to develop novel method or technology to reduce the noble metal content or improve the working efficiency of noble metal containing catalysts. Up to now, wet impregnation is still a frequent method used in the preparation of supported catalysts due to its simple operation and low cost, even if noble metal involved [12,14,16,17]. However, the uncontrollability of morphology and size of metal particles always accompanies with the impregnation process. In this presentation, we introduce a novel in situ membrane reduction method to prepare nano-sized Rh/γ-Al_2O_3 and bimetallic AuRh/γ-Al_2O_3 catalysts with high metal dispersion. The practical process of this method involves the in situ reduction of Rh/Au ions on γ-Al_2O_3 carrier with reducing agent of $NaBH_4$. The characteristics of this method are the metal ions reduction in a flowing system and the reductant addition by membrane infiltration. The particular device and procedure related will be described in the following experimental section in detail.

The Rh only and partial substitution Au for Rh supported on γ-Al_2O_3 catalysts were prepared by the novel method and wet impregnation method for comparison, which are denoted as UAMR (Ultrasound-assisted Membrane Reduction) and IMP (Impregnation), respectively. The activities of nano-sized Rh/γ-Al_2O_3 and bimetallic AuRh/γ-Al_2O_3 catalysts for the selective catalytic reduction of NO by propylene were investigated. The results showed the NO and propylene conversions were higher over the catalysts prepared by UAMR method at relatively low temperature than over those prepared by IMP method. Ueda et al. [28] have studied that the catalytic performances of Al_2O_3 supported Au catalyst for the SCR of NO by propylene. The temperature with the maximal NO conversion over 0.5 wt% Au/Al_2O_3 catalyst was ca. 400 °C. In this presentation, the activity of the catalyst was enhanced as the novel UAMR method was employed to prepare the catalyst and partial Au was substituted by Rh.

2. Experimental

2.1. Catalyst preparation

The schematic device of the UAMR process developed in our laboratory is shown in Fig. 1. For typical synthesis procedure, 4.975 g of ultra-fine γ-Al_2O_3 powder (S_{BET} = 200 $m^2\,g^{-1}$) was added to 300 ml of deionized water to form a suspension under vigorous stirring (Beaker I). An aqueous solution of $RhCl_3$ and/or H_2AuCl_4 with desired amount (corresponding 0.5 wt% loading) was then added to the γ-Al_2O_3 suspension to mix homogenously. Turn on the peristaltic pump (Baoding Lange Co., Ltd.) and set to 300 rpm ($\sim$540 ml min^{-1}) to make a tubal cycle flowing of γ-Al_2O_3 suspension mixed with the metal ions. A reductant solution (Beaker II) prepared by dissolving a quantity of $NaBH_4$ (moral ratio of 15:1 to metal) in 50 ml of deionized water was injected to the membrane reactor by using a constant flowing pump (HLB-2020, Satellite Manufactory of Beijing) with the flow rate of 1.0 ml min^{-1}. The reactor composed of three ceramic membrane tubes (Ø 3 mm × 160 mm, Hyflux Group of Companies, Singapore) with one canular glass tube outside. The Al_2O_3 suspension with metal ions flowed between the glass tube and the ceramic tubes. The $NaBH_4$ solution entered the ceramic tubes and infiltrated out through the abundant membrane holes in the tube wall. The reduction of metal ions by $NaBH_4$ immediately happened when two solutions encountered, generating the metal clusters or particles that were in situ deposited on the Al_2O_3 surface and brought away from the reaction region quickly to avoid aggregation.

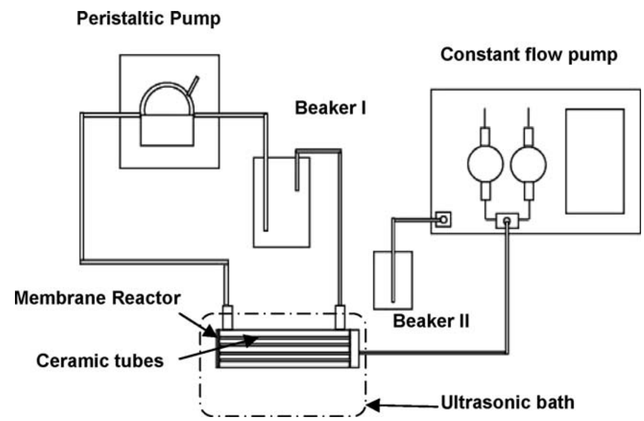

Fig. 1. Schematic diagram of Ultrasound-assisted Membrane Reduction (UAMR) device for the preparation of supported metal catalyst.

The resulting suspension was aged for 2 h under stirring after complete consumption of the $NaBH_4$ reductant solution. Then the suspension was filtrated and the resulting solid was washed with deionized water until Cl^- was not detected. The sample was dried and calcined at 500 °C for 2 h in air. The Rh/γ-Al_2O_3 and AuRh/γ-Al_2O_3 catalysts prepared by UAMR method are denoted as Rh/γ-Al_2O_3-UAMR and AuRh/γ-Al_2O_3-UAMR, respectively. No Na^+ ions were detected by XPS on the surface of the catalysts prepared with UAMR, thus the promotional effect of alkalis on DeNO_x activity can be ignored [16].

For comparison, wet impregnation method was also used to prepare Rh/γ-Al_2O_3 and AuRh/γ-Al_2O_3 catalysts, which were named as Rh/γ-Al_2O_3-IMP and AuRh/γ-Al_2O_3-IMP, with $RhCl_3$ and H_2AuCl_4 as metal precursors. In a typical synthesis, an aqueous solution of $RhCl_3$ and/or H_2AuCl_4 with a desired amount (total 0.025 g metal) was diluted to same volume with 4.975 g of γ-Al_2O_3 powder (S_{BET} = 200 $m^2\,g^{-1}$) and mixed for impregnation. The mixture was heated at 80 °C for 12 h in an oven and then calcined at 500 °C for 2 h in air at a muffle furnace. For all catalysts prepared by both methods, the Rh metal loading was 0.5 wt% for Rh/γ-Al_2O_3 catalysts. The molar ratio of 1:1 was adopted for bimetallic AuRh/γ-Al_2O_3 catalysts with total metal loading of 0.5 wt% (namely 0.33 wt% of Au and 0.17 wt% of Rh).

Generally, the catalyst was crushed and sieved into 40–60 mesh and pretreated in 10 vol.% H_2/He with total flow rate of 50 ml min^{-1} for 0.5 h at 500 °C before various measurements.

2.2. Catalytic activity

The catalytic performances of the prepared catalysts for the SCR of NO by propylene were investigated in a fixed bed quartz reactor in the temperature range of 200–500 °C. Feed gas composition was NO (0.1%), C_3H_6 (0.1%) and O_2 (5 or 1%) with He as balance at

atmospheric pressure. The mass of catalyst loaded to the reactor was 50 mg and the total flow rate of the feed gas was maintained at 100 ml min^{-1}, which corresponds to a space velocity of 120 000 h^{-1}. The reactants and products were analyzed on-line with a gas chromatograph (Shimadzu GC-2010) and a chemiluminescent NO_x analyzer (MODEL 8840) from MONITOR LABS Inc. The C_3H_6 was analyzed by using a capillary column (Rtx-1) and an FID detector. The N_2 and O_2 were analyzed by a 5A molecular sieve packed column and a TCD detector. The NO and NO_2 were analyzed by NO_x analyzer. Due to the low concentration of reactants and products in the gas flow, the volumetric change after reaction was ignored in calculation. Thus the conversions of C_3H_6 and NO as well as the NO conversion to N_2 were calculated as follows.

$$X_{C_3H_6}\,(\%) = \left(1 - \frac{[C_3H_6]_{out}}{[C_3H_6]_{in}}\right) \times 100 \tag{1}$$

$$X_{NO}\,(\%) = \left(1 - \frac{[NO]_{out}}{[NO]_{in}}\right) \times 100 \tag{2}$$

$$X_{NO \rightarrow N_2}\,(\%) = \frac{2 \times [N_2]_{out}}{[NO]_{in}} \times 100 \tag{3}$$

2.3. Characterizations

The BET surface area was determined through N_2 adsorption/desorption measurement on ASAP 2020 apparatus from Micromeritics. The samples were pretreated at 300 °C under vacuum for 5 h. Calculation of the specific surface area (BET method) was performed with the software of the apparatus.

The metal dispersion was measured by O_2–H_2 titration on AutoChem 2920 II chemical adsorption apparatus from Micromeritics. The 0.2 g of catalyst was pretreated in 10% H_2/Ar at 350 °C for 60 min and 450 °C for 30 min. Then the gas was changed to pure He, the sample was held at 475 °C for 60 min and then cooled to room temperature (RT). The catalyst was heated up to 120 °C and treated for 30 min by switching to 20% O_2/N_2. The pulse titration of pure H_2 began after sweeping for 30 min under Ar flow. The metal dispersion, metallic surface area, and active particle size were calculated automatically with the software of the apparatus.

The high resolution transmission electron microscope (HRTEM) images were obtained on JEM-2010 transmission electronic microscope (JEOL Ltd.) with accelerating voltage of 200 kV. The samples were dispersed in ethanol under ultrasound, deposited on a carbon coated copper grid before examination.

Diffuse reflectance UV–vis spectroscopic measurement was recorded on a Shimadzu UV-2450 spectrometer. The spectra were collected at 230–800 nm referenced to $BaSO_4$.

H_2-TPR of catalysts was performed on AutoChem 2920 II chemical adsorption apparatus from Micromeritics by using a mixture of 10 vol.% H_2/Ar as reducing gas with a total flow rate of 50 ml min^{-1}. A 200 mg sample was heated from RT to 800 °C at a ramping rate of 10 °C min^{-1} after pretreatment at 500 °C for 60 min in 20 vol.% O_2/N_2 gas flow (30 ml min^{-1}). The reduction signal was recorded by a TCD detector. The reducing gas was cooled by mixture of isopropanol and liquid nitrogen to remove the water formed as the reduction product.

NO-TPD (temperature programmed desorption) was carried out in a microreactor. Before performing a NO-TPD experiment, the sample (200 mg) was first pretreated in situ in 10% H_2/He at 500 °C for 1 h, followed by cooling to room temperature in the same atmosphere and then purging with 0.5% NO/He for 30 min to adsorb NO. After purging with a He flow of 50 ml min^{-1} for 30 min, the sample was heated from 30 to 800 °C at a temperature ramp rate of 10 °C min^{-1}. The effluent gases of NO (m/z = 30), O_2 (m/z = 32), N_2 (m/z = 28), N_2O (m/z = 44) and NO_2 (m/z = 46) in NO-TPD process were monitored on-line by a quadrupole mass spectrometer (HIDEN HPR20 equipped with a Faraday Cup detector and a SEM detector).

3. Results and discussions

A new concept and method, Ultrasound-assisted Membrane Reduction, was introduced to prepare fine γ-Al_2O_3 supported monometallic Rh and bimetallic AuRh catalysts with the purpose of improving the catalytic activity and decreasing the precious Rh content (then the cost) of catalyst, because of the extraordinary higher price of Rh than other noble metals such as Pt, Pd and Au. The goals are expected to achieve by preparing highly dispersed, nano-sized metal catalyst and replacing a portion of Rh with gold while preserving the activities in the meantime.

3.1. De-NO_x performance of Rh and bimetallic AuRh catalysts under lean-burn conditions

The catalytic performance of Rh/γ-Al_2O_3 and AuRh/γ-Al_2O_3 catalysts for the SCR of NO in 5% excess oxygen in feed gases are summarized in Fig. 2a–c , where the conversions of propylene and NO as well as the NO conversion to N_2 are plotted as functions of reaction temperature. Quite different catalytic behaviors over the four catalysts are observed. From Fig. 2a, one can see that the conversion of propylene over AuRh/γ-Al_2O_3-UAMR catalyst started from ca. 200 °C and increased sharply with reaction temperature increasing between 250 and 310 °C till a complete conversion at ca. 350 °C. The light-off temperature of propylene conversion ($X_{C_3H_6}$ = 50%) over Rh/γ-Al_2O_3-UAMR was ca. 340 °C that was much higher than that over AuRh/γ-Al_2O_3-UAMR (ca. 290 °C). The Rh/γ-Al_2O_3-IMP and AuRh/γ-Al_2O_3-IMP catalysts possessed relative low activities for propylene conversion with light-off temperatures of 370 and 375 °C, respectively. The NO conversions with respect to reaction temperature are presented in Fig. 2b. For all investigated catalysts, the conversions of NO reached a maximum value of 35–40% except a relatively low value of 30% for AuRh/γ-Al_2O_3-IMP with elevation of temperature and then progressively decreased as the temperature further increased. The catalytic activity for NO conversion over different catalysts according to the temperature at the maximum NO conversion decreased in the order of AuRh/γ-Al_2O_3-UAMR (310 °C) > Rh/γ-Al_2O_3-UAMR (370 °C) > Rh/γ-Al_2O_3-IMP (390 °C) > AuRh/γ-Al_2O_3-IMP (410 °C). The same order and value for the temperature corresponding to maximum NO conversion to N_2 obtained over the catalysts are presented in Fig. 2c. However, the AuRh/γ-Al_2O_3-UAMR catalyst exhibited the lowest NO conversion of 12% to N_2, whereas the conversions of NO to N_2 over other catalysts were in the range of 20–30%.

The catalytic performance of Rh/γ-Al_2O_3 and AuRh/γ-Al_2O_3 catalysts in 1% excess oxygen in feed gases are presented in Fig. 3a–c, in which the conversions of propylene and NO as well as the NO conversion to N_2 are also plotted as functions of reaction temperature. It can be seen from Figs. 2 and 3 that there was no significant difference on propylene conversion no matter the O_2 concentration was 1 or 5% in feed gas flow for all samples except the AuRh/γ-Al_2O_3-IMP catalyst, over which the propylene conversion of 100% was obtained at ca. 500 °C. For conversion of NO, the AuRh/γ-Al_2O_3-UAMR showed superior activity with a maximum NO conversion of 37% at relatively low temperature of 330 °C to other catalysts that gave the maximum NO conversion around 25% at relatively higher temperature. The maximum conversions of NO to N_2 were also obtained over the four catalysts at different reaction temperatures. However, all maximum values were below 20% that were lower than the values in the case of 5% excess oxygen in feed gas flow. Mendioroz et al. [29] also found

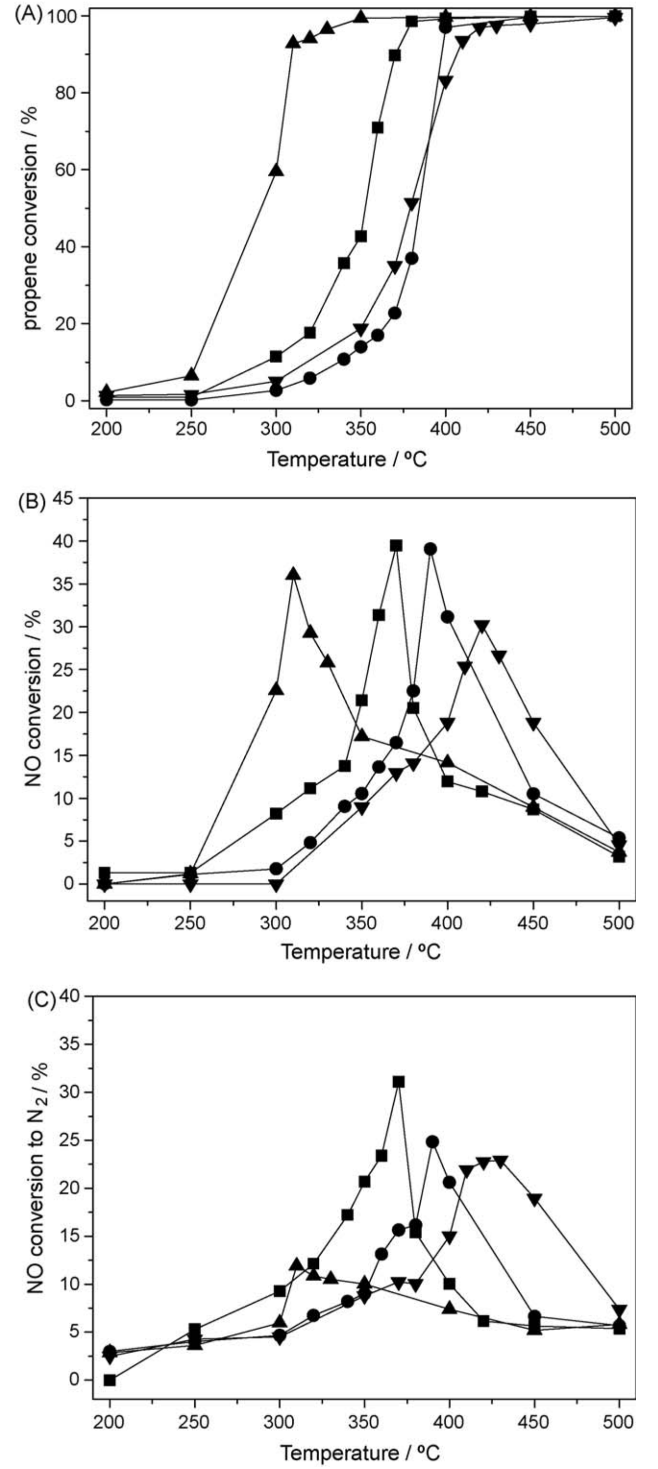

Fig. 2. Conversions of propylene (a) and NO (b) as well as the NO conversion to N_2 (c) over Rh/γ-Al_2O_3-UAMR (■), Rh/γ-Al_2O_3-IMP (●), AuRh/γ-Al_2O_3-UAMR (▲) and AuRh/γ-Al_2O_3-IMP (▼) catalysts as functions of reaction temperature. Feed composition: 0.1% NO, 0.1% C_3H_6 and 5% O_2 (He as balance). SV = 120 000 h^{-1}.

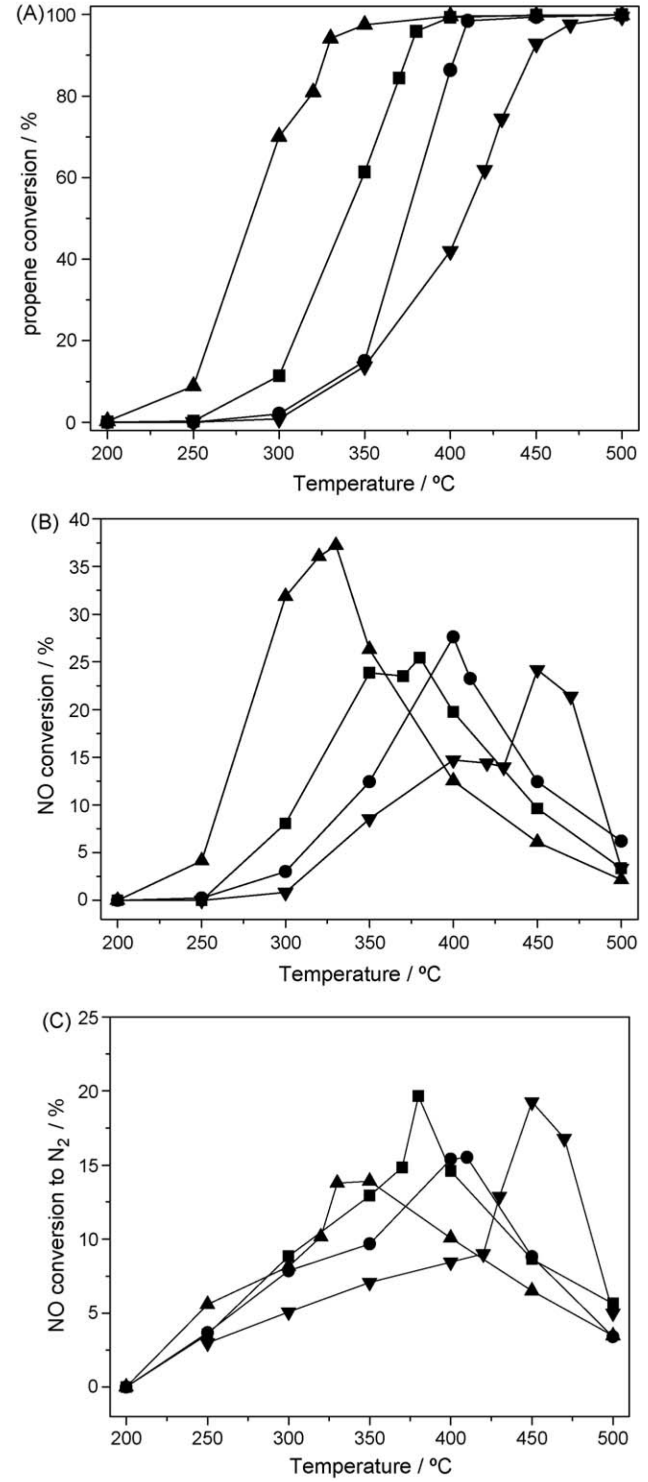

Fig. 3. Conversions of propylene (a) and NO (b) as well as the NO conversion to N_2 (c) over Rh/γ-Al_2O_3-UAMR (■), Rh/γ-Al_2O_3-IMP (●), AuRh/γ-Al_2O_3-UAMR (▲) and AuRh/γ-Al_2O_3-IMP (▼) catalysts as functions of reaction temperature. Feed composition: 0.1% NO, 0.1% C_3H_6 and 1% O_2 (He as balance). SV = 120 000 h^{-1}.

that the NO_x conversion increased with O_2 concentration in the SCR of NO_x by methane over Rh-based aluminium pillared clays. It is similar to our results. The role of oxygen is crucial to the formation of surface Rh–NO_2 species over Rh-based catalysts, which further reacts with hydrocarbons adsorbed and activated with oxygen to give N_2 and CO_2. The increase of O_2 partial pressure favors the formation of adsorbed NO_2 and thus improvement of NO_x conversion and N_2 selectivity.

Very similar catalytic performances for the reduction of NO by propylene without oxygen in feed gas were observed over the four different catalysts and only the result of AuRh/γ-Al_2O_3-UAMR catalyst is shown in Fig. 4. One can see that the NO in feed could be reduced completely by propylene in the absence of oxygen above 350 °C. The conversion of propylene was below 20% due to the lack of oxidant in the reaction system. The NO conversion to N_2 increased progressively up to ca. 50% with a rise in temperature.

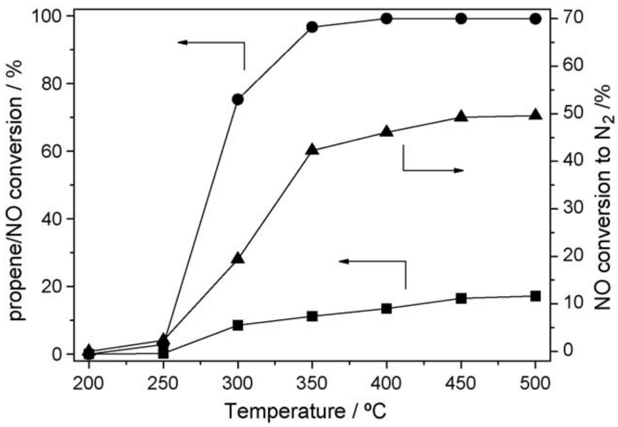

Fig. 4. Conversions of propylene (■) and NO (●) as well as the NO conversion to N_2 (▲) over AuRh/γ-Al_2O_3-UAMR catalyst as functions of reaction temperature. Feed composition: 0.1% NO, 0.1% C_3H_6 (He as balance). SV = 120 000 h^{-1}.

From above catalytic test results, the catalysts prepared by novel UAMR method exhibited higher activities than the catalysts prepared by conventional IMP method under the same reaction conditions. The bimetallic AuRh/γ-Al_2O_3-UAMR catalyst demonstrated the highest activity for NO reduction when propylene was used as reductant at low temperature. However, the AuRh/γ-Al_2O_3-IMP showed the lowest activity under the same conditions, indicating that the preparation method was very important to determine the activity of the catalysts. To take account of propylene and NO conversions, the activities of the catalysts decreased as: AuRh/γ-Al_2O_3-UAMR > Rh/γ-Al_2O_3-UAMR > Rh/γ-Al_2O_3-IMP > AuRh/γ-Al_2O_3-IMP. If the 0.5 wt% AuRh/γ-Al_2O_3 ($m_{Au/Rh}$ = 1) was substituted for 0.5 wt% Rh/γ-Al_2O_3, the Rh loading on catalyst could be reduced by 66% in weight.

3.2. Metal dispersion

Some physico-chemical properties of Rh/γ-Al_2O_3 and AuRh/γ-Al_2O_3 catalysts prepared by both methods are presented in Table 1. It could be found that the surface area of catalysts prepared by UAMR almost preserved compared with blank γ-Al_2O_3 support (~200 m^2 g^{-1}). The catalysts prepared by IMP method showed a little decrease of surface area. It may originate from the light sintering in the hot impregnation and next calcination process. The actual metal content determined by ICP-OES was also listed in Table 1. It could be found that the values of all actual metal content were less than the corresponding theoretical values and there were not significant differences in the actual metal contents for the catalysts prepared by both methods, indicating the loss of metal when the UAMR method was employed was not bigger than that in the case of the wet impregnation method used.

It has been shown recently that bulk Au is chemically inert and no obvious adsorption of H_2 and O_2 on Au surface was observed [30]. On the other hand, the small Au clusters are catalytically active and can adsorb/dissociate O_2 and H_2 [30,31], but the dependence of adsorption activity on cluster size is not well understood. To include much possible situation (such as partial Au atoms involved in the adsorption of O_2 and H_2), the metal dispersion of bimetallic AuRh/γ-Al_2O_3 catalyst determined by O_2–H_2 titration was calculated based on both exclusive Rh metal and bimetallic AuRh with the software of apparatus. In Table 1, the high metal dispersions were obtained on the catalysts prepared by UAMR method (45.3% for Rh/γ-Al_2O_3 and 74.5/40.1% for AuRh/γ-Al_2O_3), while the metal dispersions on catalysts prepared by IMP method were absolutely lower (6.2% and 11.1/6.3% for Rh and AuRh catalysts, respectively). Similarly, the metallic surface area (both sample and metal based) and active particle diameter were calculated. Relatively higher metallic surface area and smaller particle size could be obtained on catalysts by UAMR, suggesting the UAMR method was favorable for improving metal dispersion and reducing mean crystalline size. It consequently benefited the adsorption and activation of reactant molecules and improved catalytic activity. The lowering of C_3H_6 and NO conversion temperature in NO-SCR for catalysts by UAMR compared to IMP method confirmed the superiority of the resulting higher metal dispersion and smaller crystalline size by UAMR method.

3.3. High resolution transmission electron microscopy

Before electron microscopy investigation, all samples were subjected to reduction treatment in a hydrogen flow. The HRTEM overviews of the four catalysts are given in Fig. 5. All lengths of the scale on the figures are 5 nm. From the images, it might be recognized that highly dispersed metal particles with nanometer size in the range of 2–10 nm were produced. Typically, the size of Rh nanoparticles on Rh/γ-Al_2O_3-UAMR catalyst was ca. 2–5 nm in diameter (Fig. 5a), whereas bimetallic AuRh/γ-Al_2O_3-UAMR catalyst exhibited larger metal nanoparticles of 3–7 nm, which might be composed of AuRh alloy or core/shell structure by co-reduction (not visualized in Fig. 5c). Generally, the catalysts prepared by conventional impregnation method exhibited larger metal particle range from 5 to 20 nm or bigger as agglomerated particles (Fig. 5b and d). The observations were comparable to the calculation results of active particle size in the metal dispersion measurement. The smaller metal nanoparticles could supply higher metal surface, more surface atoms and active sites, from which the advantages of catalysts prepared by UAMR method might arise. These results revealed the advantages of the UAMR method for the preparation of highly dispersed mono- or bimetallic nanocatalysts.

3.4. Diffuse reflection UV–vis spectra of bimetallic AuRh/γ-Al_2O_3 catalysts

Since metallic Rh do not adsorb UV-visible light [32], the AuRh/γ-Al_2O_3 catalysts prepared by UAMR and IMP methods were

Table 1
Physico-chemical properties of Rh/Al_2O_3 and AuRh/Al_2O_3 catalysts.

Catalyst	Surface area (m^2/g)	Metal content (wt%) actual/nominal		Metal dispersion (%)'	Metallic surface area		Active particle diameter (nm)
		Au	Rh		m^2/g sample	m^2/g metal	
Rh/γ-Al_2O_3-UAMR	196.6	–	0.40/0.50	45.3	0.80	199.6	2.4
Rh/γ-Al_2O_3-IMP	180.6	–	0.37/0.50	6.2	0.10	27.1	17.8
AuRh/γ-Al_2O_3-UAMR	199.7	0.23/0.33	0.14/0.17	74.5[a]/40.1[b]	0.46/0.49	327.8/133.0	1.5/2.9
AuRh/γ-Al_2O_3-IMP	186.0	0.22/0.33	0.15/0.17	11.1[a]/6.3[b]	0.07/0.08	48.7/21.1	9.9/18.5

[a] Calculated based on Rh only.
[b] Calculated based on AuRh; the same to metallic surface area and active particle diameter.

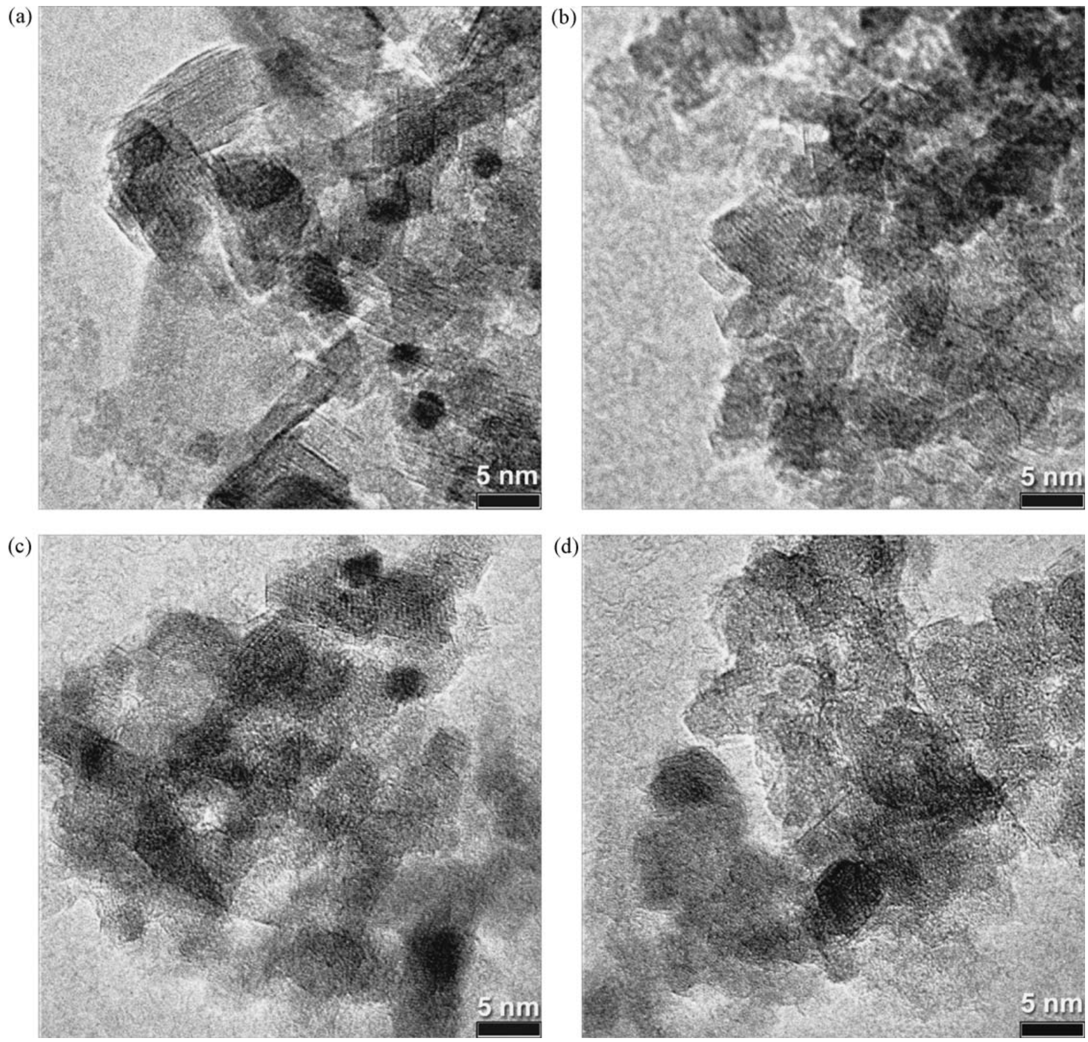

Fig. 5. The HRTEM images of Rh/γ-Al_2O_3-UAMR (a), Rh/γ-Al_2O_3-IMP (b), AuRh/γ-Al_2O_3-UAMR (c), and AuRh/γ-Al_2O_3-IMP (d) samples.

studied by diffuse reflection UV–vis to identify the chemical state of gold. Fig. 6 shows the optical spectra of the two catalysts. The UV–vis spectrums of the both catalysts show a band of the plasmon resonance of metallic gold centered at ca. 560 nm. This plasmon absorption arises from the collective oscillations of the free conduction band electrons that are induced by the incident electromagnetic radiation. Such resonances can be observed when the wavelength of the incident light far exceeds the particle diameter [33]. Other additional absorption bands contributed to ionic gold or partly charged Au nanoclusters were not detected in the optical spectra (absorption bands below 500 nm) [34]. From Fig. 6, one can see that the AuRh/γ-Al_2O_3-UAMR catalyst possessed a broader absorption band and larger full width at half-maximum (FWHM) than the AuRh/γ-Al_2O_3-IPM catalyst, implying that the metal particles on the former catalyst were smaller than those on the latter sample [34]. The experimental results were in good agreement with the observation of HRTEM. However, the relation between the mean particle diameter, the peak position and the FWHM is also influenced by the surrounding environment and the interaction between the gold particles and the support [35,36].

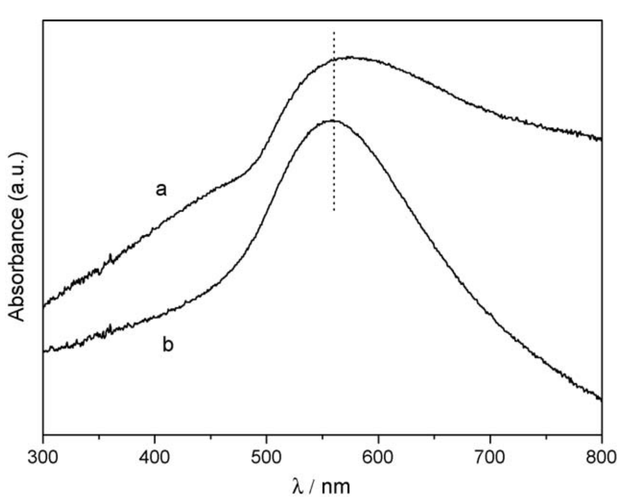

Fig. 6. DR UV–vis spectra of AuRh/γ-Al_2O_3-UAMR (a) and AuRh/γ-Al_2O_3-IMP (b) catalysts.

3.5. H_2-TPR

The H_2-TPR profiles of the catalysts are presented in Fig. 7. A peak centered at 102 and 92 °C was observed for Rh/γ-Al_2O_3 catalysts prepared by UAMR and IMP methods, respectively, which can be attributed to the reduction of RhO_x to Rh [37–39]. This reduction peak also appeared with lower intensity and temperature for bimetallic AuRh/γ-Al_2O_3 catalysts prepared by both UAMR and IMP methods. It is understandable that the Rh content (0.17 wt%) of AuRh/γ-Al_2O_3 is much less than that of Rh/γ-Al_2O_3

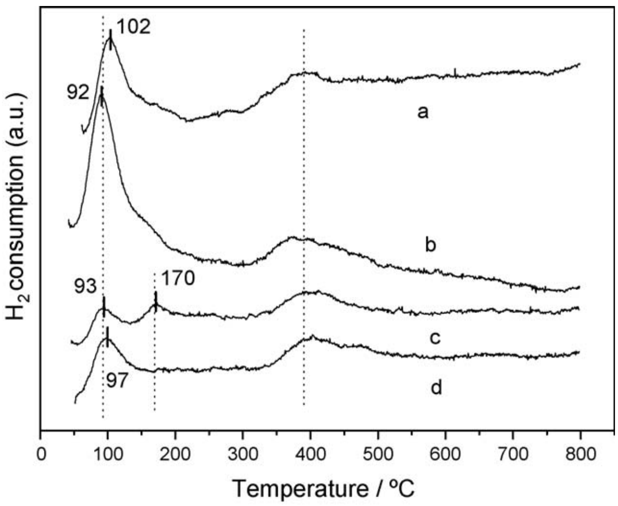

Fig. 7. H_2-TPR profiles of Rh/γ-Al_2O_3-UAMR (a), Rh/γ-Al_2O_3-IMP (b), AuRh/γ-Al_2O_3-UAMR (c) and AuRh/γ-Al_2O_3-IMP (d) catalysts.

(0.5 wt%). For the AuRh/γ-Al_2O_3-UAMR catalyst, another reduction peak was observed at 170 °C that can be assigned to the reduction of Au_xO_y gold species [40] or the oxygen species on the fine gold particles [41,42]. Liu and Yang [43] have found that 1.6 wt% Au/Al_2O_3 showed a gold species reduction peak at 177 °C, which was similar to our present result. However, the AuRh/γ-Al_2O_3-IMP catalyst did not exhibit clear reduction peak related to gold. This reflected that the reducibility or surface adsorption ability changed when the UAMR novel method was employed to fabricate the catalyst. In addition, it is noteworthy that a broad reduction peak at ca. 400 °C could be observed for all the catalysts investigated, which can be assigned to the reduction of the rhodium oxide species that intimately interacted with the Al_2O_3 surface (RhO_x) or the surface $Rh(AlO_2)_y$ species formed by diffusion of rhodium oxides into sublayers of Al_2O_3 structure as a result of high temperature oxidation since the bulk $Rh(AlO_2)_y$ species need to be reduced at higher temperature above 500 °C [44,45].

3.6. NO-TPD

All catalysts were pretreated in 10 vol.% H_2/He gas flow at 500 °C for 30 min before temperature programmed desorption experiments. The NO-TPD profiles of the four catalysts are presented in Fig. 8. The corresponding analytical and quantitative results are summarized and listed in Table 2.

According to the previous investigation of other researchers [46–49], there were three types of adsorbed NO_x species corresponding to nitrosyl, nitrite, and nitrate species with desorption peak temperatures of ca. 100, 270 and 460 °C, respectively. From Fig. 8a and b, Rh/γ-Al_2O_3-UAMR and Rh/γ-Al_2O_3-IMP catalysts exhibited only one NO desorption peak at 133 and 170 °C, respectively, on the TPD profile. This result is different from the observation made by Burch et al. [46,47] and Kotsifa et al. [49] since they found that the Al_2O_3 support could give peak of NO desorption at elevated temperature independently. Li et al. [45] reported that there was a strong metal–support interaction (SMSI) between Rh and Al_2O_3. The SMSI effect decreased the NO adsorption and formation of nitrates. Therefore, no obvious O_2 desorbed was detected through the whole temperature region. However, quite different NO desorption behaviors were observed

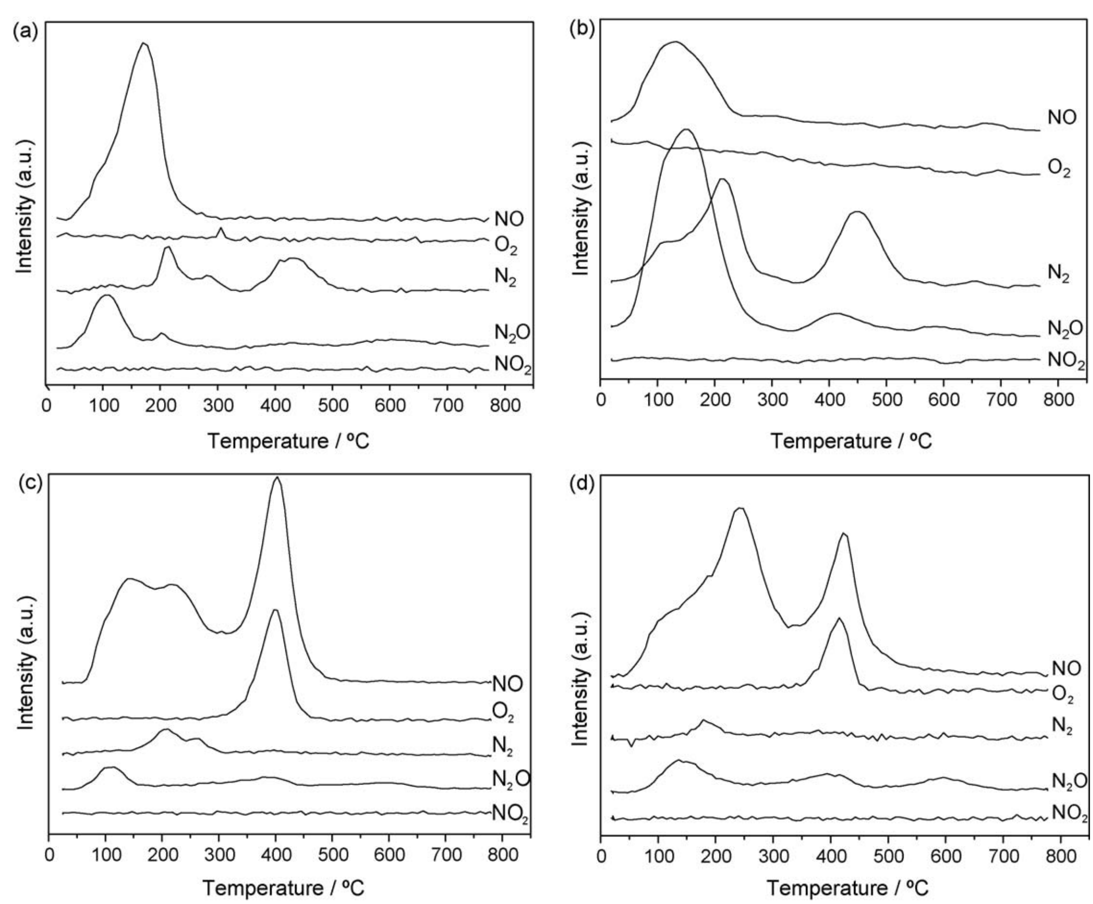

Fig. 8. NO-TPD profiles of Rh/γ-Al_2O_3-UAMR (a), Rh/γ-Al_2O_3-IMP (b), AuRh/γ-Al_2O_3-UAMR (c) and AuRh/γ-Al_2O_3-IMP (d) catalysts.

Table 2
Peak temperature and quantities of various species desorption in NO-TPD.

	Catalyst	Rh/Al(UAMR)	Rh/Al(IMP)	AuRh/Al(UAMR)	AuRh/Al(IMP)
NO	Temp. (°C)	170	133	147, 218, 403	122, 240, 421
	A_T [a]	39	8	128	79
O_2	Temp. (°C)	–	–	397	415
	A_T [a]	–	–	26	9
N_2	Temp. (°C)	215, 280, 433	110, 217, 445	211, 257	178, 386
	A_T [a]	13	14	8	4
N_2O	Temp. (°C)	104, 201	146, 411	116, 391	135, 393, 596
	A_T [a]	15	23	14	17
	A_{NO} [b]	95	82	172	121

[a] Quantities of various species desorbed in μmol g^{-1}.
[b] $A_{NO} = A_T(NO) + 2 \times A_T(N_2) + 2 \times A_T(N_2O)$, quantities of all desorbed N-containing species counted by NO in μmol g^{-1}.

on the bimetallic AuRh/γ-Al_2O_3 catalysts (Fig. 8c and d). An obvious NO desorption at high temperature was determined accompanying with an unique O_2 desorbed peak appears at ca. 400 and 420 °C for samples prepared by UAMR and IMP methods, respectively, indicating the decomposition of some surface nitrate-type species at this temperature [46,49]. The presence of nitrate species (NO_3^-) on Au-containing catalyst after adsorption of NO was confirmed by Debeila et al. using DRIFTS studies [50,51]. Moreover, it is also observed that the NO desorption peaks at ca. 147 and 218 °C lapped over each other for the AuRh/γ-Al_2O_3-UAMR catalyst (Fig. 8c). In the case of AuRh/γ-Al_2O_3-IMP catalyst, the NO desorption peak at middle temperature of 240 °C was dominant with the NO desorption peak at low temperature of 122 °C as a shoulder (Fig. 8d). The N_2 and N_2O desorptions were always obtained with different quantities and temperatures for all catalysts. The formation of these species would be discussed as follows.

Generally, the dissociation of NO on metal catalyst and the combination of a set of surface elementary process has been widely accepted by researchers as follows. These steps should take place on the surface of both metal and support, and mostly on the metal surface [17,46,49,52,53].

$$NO + * \rightleftharpoons NO* \quad (4)$$

$$NO* \rightleftharpoons N* + O* \quad (5)$$

$$NO + O* \rightleftharpoons NO_2* \quad (6)$$

$$NO + 2O* \rightleftharpoons NO_3* \quad (7)$$

where * would represent a surface vacant site and all the steps are reversible to some extents. The absolutely reverse processes of (4) and (6) may be responsible for the NO desorption at low or medium temperature. The reverse process of (7) combined with $2O^* \rightarrow O_2$ or the direct decomposition of NO_3^* to NO and O_2 can account for the high temperature peak of NO desorption. Regarding the formation of N_2 and N_2O, Chin [52] and Hirano [53] proposed a similar mechanism as follows.

$$2N* \rightarrow N_2 + 2* \quad (8)$$

$$NO* + N* \rightarrow N_2 + O* + * \quad (9)$$

$$NO* + N* \rightarrow N_2O + 2* \quad (10)$$

However, many researchers considered that it was difficult to realize the N-pairing by surface diffusion of N atoms over highly dispersed Rh catalysts [54,55]. According to Shelef and Graham [54], the highly dispersed, supported Rh catalysts had the ability to promote the N-pairing among the adsorbed NO molecules before the N–O bond was broken. Therefore, the plausible surface reactions should contain:

$$2NO* \rightarrow N_2 + 2O* \quad (11)$$

$$2NO* \rightarrow N_2O + O* \quad (12)$$

Rahkamaa and Salmi [55] agreed this suggestion and made a modification on it. They proposed a surface mechanism based on NO adsorption and formation of a surface complex (*ON···NO*), which is decomposed to N_2 and N_2O.

Due to the nano-dispersion of present γ-Al_2O_3 supported Rh and AuRh catalysts (from metal dispersion, HRTEM and UV characterizations), the mechanisms proposed by Shelef or Rahkamaa [54,55] may be suitable for use to explain the formation of N_2 and N_2O species over the present Rh/γ-Al_2O_3 and AuRh/γ-Al_2O_3 catalysts.

The desorption behaviors of various species were very different over the catalysts (see Table 2) no matter what formation mechanism involved. The experimental results in Table 2 were briefly summarized as follows: (i) the catalysts prepared by UAMR method gave larger quantities of NO desorbed than the catalysts fabricated by IMP method (39/8 for Rh catalyst and 128/79 for AuRh catalysts), even if compared by total equivalent NO quantities (95/82 for Rh and 172/121 for AuRh); (ii) the AuRh/γ-Al_2O_3 catalysts gave larger quantities of NO desorbed than Rh/γ-Al_2O_3 catalysts for both methods (128/39 and 79/8, respectively), the same as in comparison with the total equivalent NO quantities (172/95 for UAMR and 121/82 for IMP, respectively); (iii) the number of NO desorption peaks increased from one (for Rh only catalysts) to three (for AuRh catalysts), especially the appearance of high temperature peak; (iv) the Rh/γ-Al_2O_3 catalysts gave larger quantities of N_2 and N_2O desorbed than AuRh/γ-Al_2O_3 catalysts for both preparation method (N_2: 13/8 for UAMR and 14/4 for IMP, respectively; N_2O: 15/14 for UAMR and 23/17 for IMP, respectively).

The introduction of Au atoms into the Rh-based catalyst plays an important role for preserving and improving the catalytic activity of the Rh-based catalysts. The actual role of Au in the SCR of NO might lie on the enhancement of NO adsorption abilities, which was demonstrated by the appearance of high temperature NO desorption peak and the increase of total NO desorption quantities in NO-TPD. Like Cu^+ with the same out-shell electronic structure [56], the electrons in d orbit are filled for Au atoms and their electron hole in d energy band is zero. The resulting electron donor properties increased the chemsorption bond strength of electron acceptor adsorbates (NO). Moreover, the nano-sized Au particles exhibited more under-coordinated atoms and higher surface energy to strengthen surface adsorption ability. As a result, the NO adsorption was enhanced with Au additive. However, the AuRh/γ-Al_2O_3 catalyst prepared by IMP method did not exhibit anticipated high activity. Besides the larger metal particle size of

AuRh/γ-Al_2O_3-IMP catalyst (from TEM photographs), the reducible Au (from TPR results) in AuRh/γ-Al_2O_3-UAMR catalyst made the easy participation of Au into reaction process, which promote the adsorption and dissociation of NO. It was reflected by the more desorption quantities of O_2 and N_2 species. The strong ability of adsorption and dissociation for NO could account for the high activity at low temperature of AuRh/γ-Al_2O_3-UAMR catalyst. The lower N_2 desorption quantities (formed in NO-TPD process) should have some relations with the lower values of NO conversion to N_2 (from activity test) for the AuRh/γ-Al_2O_3-UAMR catalyst. Although the AuRh/γ-Al_2O_3-IMP catalyst also showed low N_2 desorption, the higher N_2O quantities allowed some part of N_2 produced from self-decomposition of N_2O [55]. Therefore, the value of NO conversion to N_2 was not lower than other catalysts.

UAMR has been proved to be a very useful and efficient technique for preparing metal nanocatalyst with nano-dispersion. It is benefit for improving activity and constructing bimetallic AuRh/γ-Al_2O_3 catalyst system with high catalytic performance. The catalytic performances of AuRh/γ-Al_2O_3 in other probing reactions are under investigation, such as CO oxidation, CO + NO, and so on.

4. Conclusions

The supported monometallic Rh/γ-Al_2O_3 and bimetallic AuRh/γ-Al_2O_3 catalysts were prepared by a novel Ultrasound-assisted Membrane Reduction method and conventional impregnation method. The selective catalytic reduction of NO under excess oxygen over the catalysts was investigated. The high activities at lower reaction temperature were obtained over the catalysts prepared by the new UAMR method compared to the catalysts prepared by IMP method. It was attributed to the smaller metal particle size and the stronger NO adsorption capacity for both Rh/γ-Al_2O_3 and AuRh/γ-Al_2O_3 nanocatalysts prepared by UAMR method. Another important conclusion was that when partial Rh (about 66 wt%) was replaced by Au, namely the bimetallic AuRh catalyst, it preserved (even enhanced) the activity compared to the Rh only catalyst. The stronger NO adsorption capacity, especially the formation of surface nitrate species, after the introduction of Au, was observed at the same time.

Acknowledgements

The authors are grateful for the financial support of the National 863 Program Foundation of China (grant no. 2006AA06Z347) and the project (grant nos. 20877006 and 20833011) supported by the National Natural Science Foundation of China.

References

[1] V.A. Sadykov, S.L. Baron, V.A. Matyshak, G.M. Alikina, R.V. Bunina, A.Ya. Rozovskii, V.V. Lunin, E.V. Lunina, A.N. Kharlanov, A.S. Ivanova, S.A. Veniaminov, Catal. Lett. 37 (1996) 157.
[2] J. Shibata, K. Shimizu, A. Satsuma, T. Hattori, Appl. Catal. B 37 (2002) 197.
[3] T.I. Halkides, D.I. Kondarides, X.E. Verykios, Appl. Catal. B 41 (2003) 415.
[4] Z. Liu, S.I. Woo, Catal. Rev. 48 (2006) 43.
[5] H. Hamada, Y. Kintaichi, M. Tabata, M. Sasaki, T. Ito, Chem. Lett. (1991) 2179.
[6] T. Tabata, H. Ohtsuka, L.M.F. Sabatino, G. Bellussi, Micropor. Mesopor. Mater. 21 (1998) 517.
[7] F. Lónyi, J. Valyon, L. Gutierrez, M.A. Ulla, E.A. Lombardo, Appl. Catal. B 73 (2007) 1.
[8] K. Shimizu, K. Sugino, K. Kato, S. Yokota, K. Okumura, A. Satsuma, J. Phys. Chem. C 111 (2007) 6481.
[9] H. Hamada, Y. Kintaichi, M. Inaba, M. Tabata, T. Yoshinari, H. Tsuchida, Catal. Today 29 (1996) 53.
[10] T. Maunula, Y. Kintaichi, M. Inaba, M. Haneda, K. SatoL, H. Hamada, Appl. Catal. B 15 (1998) 291.
[11] Q.C. Lin, J.M. Hao, J.H. Li, Z.F. Ma, W.M. Lin, Catal. Today 126 (2007) 351.
[12] T.I. Halkides, D.I. Kondarides, X.E. Verykios, Catal. Today 73 (2002) 213.
[13] G.E. Marnellos, E.A. Efthimiadis, I.A. Vasalos, Appl. Catal. B 48 (2004) 1.
[14] K. Arve, H. Backman, F. Klingstedt, K. Eränen, D.Y. Murzin, Appl. Catal. A 303 (2006) 96.
[15] H. Backman, K. Arve, F. Klingstedt, D.Y. Murzin, Appl. Catal. A 304 (2006) 86.
[16] I.V. Yentekakis, V. Tellou, G. Botzolaki, I.A. Rapakousios, Appl. Catal. B 56 (2005) 229.
[17] A. Kotsifa, D.I. Kondarides, X.E. Verykios, Appl. Catal. B 80 (2008) 260.
[18] J.N. Armor, Catal. Today 26 (1995) 147.
[19] M.D. Amiridis, T. Zhang, R.J. Farrauto, Appl. Catal. B 10 (1996) 203.
[20] A. Fritz, V. Pitchon, Appl. Catal. B 13 (1997) 1.
[21] V.I. Pârvulescu, P. Grange, B. Delmon, Catal. Today 46 (1998) 233.
[22] Y. Traa, B. Burger, J. Weitkamp, Micropor. Mesopor. Mater. 30 (1999) 3.
[23] R. Burch, J.P. Breen, F.C. Meunier, Appl. Catal. B 39 (2002) 283.
[24] J.P. Breen, R. Burch, Top. Catal. 39 (2006) 53.
[25] K. Shimizu, M. Tsuzuki, A. Satsuma, Appl. Catal. B 71 (2007) 80.
[26] R.M. Heck, R.J. Farrauto, Appl. Catal. A 221 (2001) 443.
[27] J. Kašpar, P. Fornasiero, N. Hickey, Catal. Today 77 (2003) 419.
[28] A. Ueda, T. Oshima, M. Haruta, Appl. Catal. B 12 (1997) 81.
[29] S. Mendioroz, A.B. Martín-Rojo, F. Rivera, J.C. Martín, A. Bahamonde, M. Yates, Appl. Catal. B 64 (2006) 161.
[30] G.C. Bond, C. Louis, D.T. Thompson, Catalysis by Gold, Imperial College Press.
[31] G. Mills, M.S. Gordon, H. Metiu, J. Chem. Phys. 118 (2003) 4198.
[32] K. Sato, T. Yoshinari, Y. Kintaichi, M. Haneda, H. Hamada, Appl. Catal. B 44 (2003) 67.
[33] M. Lamallem, H. El Ayadi, C. Gennequin, R. Cousin, S. Siffert, F. Aïssi, A. Aboukaïs, Catal. Today 137 (2008) 367.
[34] A.C. Gluhoi, N. Bogdanchikova, B.E. Ieuwenhuys, J. Catal. 229 (2005) 154.
[35] A.C. Gluhoi, N. Bogdanchikova, B.E. Ieuwenhuys, J. Catal. 232 (2005) 96.
[36] P. Claus, A. Brückner, C. Mohr, H. Hofmeister, J. Am. Chem. Soc. 122 (2000) 11430.
[37] H. He, H.X. Dai, L.H. Ng, K.W. Wong, C.T. Au, J. Catal. 206 (2002) 1.
[38] J.X. Guo, M.C. Gong, S.H. Yuan, Y.Q. Chen, J. Rare Earth 24 (2006) 554.
[39] S. Eriksson, S. Rojas, M. Boutonnet, J.L.G. Fierro, Appl. Catal. A 326 (2007) 8.
[40] F.-W. Chang, S.-C. Lai, L.S. Roselin, J. Mol. Catal. A 282 (2008) 129.
[41] D. Andreeva, V. Idakiev, T. Tabakova, L. Ilieva, P. Falaras, A. Bourlinos, A. Travlos, Catal. Today 72 (2002) 51.
[42] M.-A. Hurtado-Juan, C.M.Y. Yeung, S. Chi Tsang, Catal. Commun. 9 (2008) 1551.
[43] S.Y. Liu, S.M. Yang, Appl. Catal. A 334 (2008) 92.
[44] C.-P. Hwanga, C.-T. Yeh, Q. Zhu, Catal. Today 51 (1999) 93.
[45] J.M. Li, F.Y. Huang, W.Z. Weng, X.Q. Pei, C.R. Luo, H.Q. Lin, C.J. Huang, H.L. Wan, Catal. Today 131 (2008) 179.
[46] R. Burch, E. Halpin, J.A. Sullivan, Appl. Catal. B 17 (1998) 115.
[47] R. Burch, J.A. Sullivan, T.C. Watling, Catal. Today 42 (1998) 13.
[48] S. Benard, L. Retailleau, F. Gaillard, P. Vernoux, A. Giroir-Fendler, Appl. Catal. B 55 (2005) 11.
[49] A. Kotsifa, D.I. Kondarides, X.E. Verykios, Appl. Catal. B 72 (2007) 136.
[50] M.A. Debeila, N.J. Coville, M.S. Scurrell, G.R. Hearne, J. Mol. Catal. A 219 (2004) 131.
[51] M.A. Debeila, N.J. Coville, M.S. Scurrell, G.R. Hearne, Appl. Catal. A 291 (2005) 98.
[52] A.A. Chin, A.T. Bell, J. Phys. Chem. 87 (1983) 3700.
[53] H. Hirano, T. Yamada, K.I. Tanaka, J. Siera, P. Cobden, B.E. Nieuwenhuys, Surf. Sci. 262 (1992) 97.
[54] M. Shelef, G.W. Graham, Cat. Rev. Sci. Eng. 36 (1994) 433.
[55] K. Rahkamaa, T. Salmi, Chem. Eng. Sci. 54 (1999) 4343.
[56] J. Datka, E. Kukulska-Zajac, W. Kobyzewa, Catal. Today 114 (2006) 169.